PARALLEL AND DISTRIBUTED SYSTEMS LABORATORY

Solving Partial Differential equations on adaptive point clouds

A part of an open source meshless project **Medusa**
https://gitlab.com/e62Lab/medusa
http://e6.ijs.si/medusa/

Department of Communications Systems
Institute "Jožef Stefan"
Jamova 39, 1000 Ljubljana, Slovenia

Gregor Kosec
Jožef Stefan Institute, Slovenia

Università degli Studi di Trieste, Dipartimento di Ingegneria e Architettura, 2024

Jožef Stefan Institute

Basic info

Leading Slovenian research organization

The Jožef Stefan Institute is named after the distinguished 19th century physicist Jožef Stefan, most famous for his work on the Stefan-Boltzmann law of black-body radiation and Stefan's problems (study of ice growth)

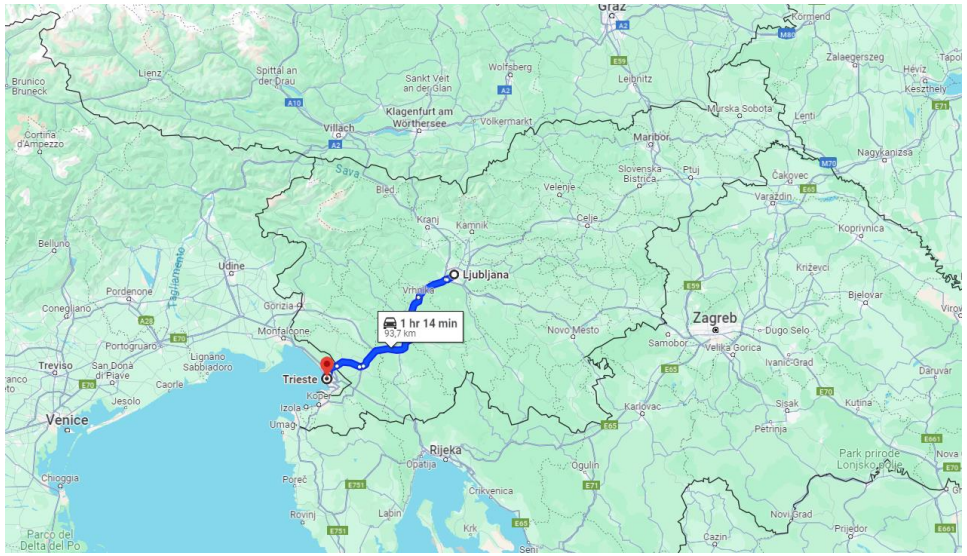

JSI HQ in Ljubljana, Jamova cesta 39

IJS Reactor Center Podgorica

JSI in numbers

- 1200 employees
- Revenue approximately - 85 M€
- 60 % national programme – 10 % applied research - 10 % international projects – 20 % industrial contracts
- 430+ ongoing national and international projects

Jožef Stefan Institute

Basic info

There are three main research branches at JSI

Physics:

- Theoretical Physics
- Low and Medium Energy Physics
- Thin Films and Surfaces,
- Surface Engineering and Optoelectronics,
- Condensed Matter Physics,
- Complex Matter, Reactor Physics,
- Experimental Particle Physics

Electronics and Information Technologies

- Automation,
- Bio-cybernetics and Robotics,
- Systems and Control,
- Artificial Intelligence,
- Open Computer Systems and Networks,
- Communication Systems (P-Lab)
- Computer Systems,
- Knowledge Technologies,
- Intelligent Systems

Chemistry and Biochemistry:

- Biochemistry and Molecular Biology
- Molecular and Biomedical Sciences,
- Biotechnology,
- Inorganic Chemistry and Technology,
- Electronic Ceramics, Engineering Ceramics,
- Nanostructured Materials,
- Synthesis of Materials,
- Advanced Materials
- Environmental Sciences

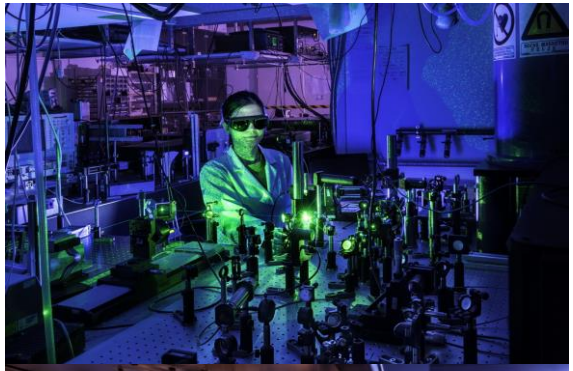

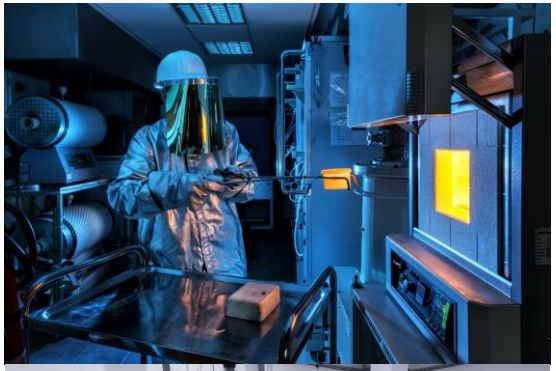

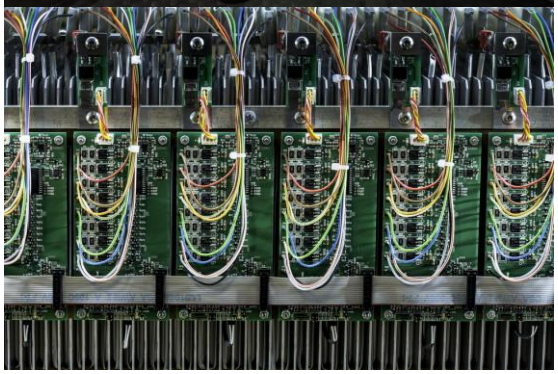
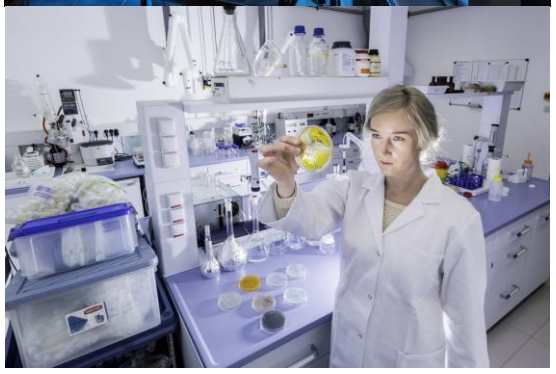

Parallel and distributed systems laboratory

One of three Laboratories from Communication Systems department

Team: 6 full time researchers (3 PhD students) :: 2 part time researches :: 1 technician :: 7 MSc students

Interested in: Scientific computing.

Active projects

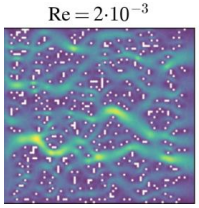

Inertial effects on fluid flow in complex porous media (NCN-ARRS)

Advanced concept of efficient use of transformers leveraging the DTR technology (Applied)

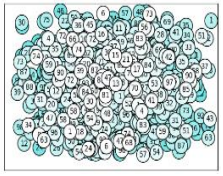

Cryptographically secure random number generator(Applied)

Advanced modelling of radio channels using meshless methods (ARRS)

AiCoachU – Artificial intelligence is coaching you (ARRS)

Modelling the Decay of an invasive ctenophore blooms (ARRS)

Past climate change and glaciation at the Alps-Dinarides junction(ARRS)

DiTeR: Dynamic thermal line rating of power lines (Applied)

Forecasting tap changer regulatory maintenance with advanced analytics (Applied)

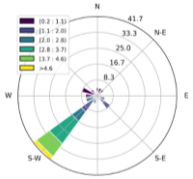

Downscaling meteorological variables over complex terrain(applied)

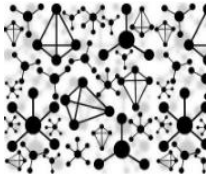

Graph Theory and Combinatorial Scientific Computing (OTKA-ARRS)

Holistic Approach towards Empowerment of the DiGitalization of the Energy Ecosystem(HE)

Meshless numerical methods for solving PDEs

We want to solve PDEs

$$\rho\frac{\partial \mathbf{v}}{\partial t}+\rho\nabla\cdot(\mathbf{vv})=-\nabla P+\nabla\cdot\left(\mu\nabla\mathbf{v}\right)+\mathbf{b}$$

$$\rho\frac{\partial\left(c_pT\right)}{\partial t}+\rho\nabla\cdot(c_pT\mathbf{v})=\nabla\cdot\left(\lambda\nabla T\right)$$

... that do not have closed form solution.

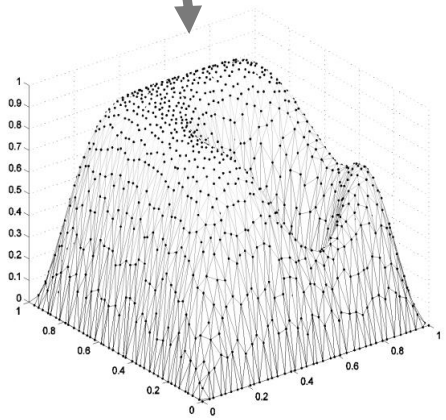

Employ numerical method to transform PDE to the system of algebraic equations

Discretize the domain into final number of elements or nodes.

Approximate partial differential operator

Approximate PDE resulting in a linear system

Solve the linear system

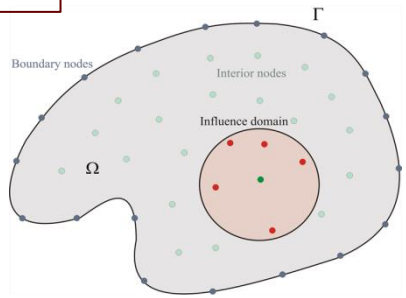

Meshless methods
RBF-FD, MLPG, DAM, LRBFCM, SPH

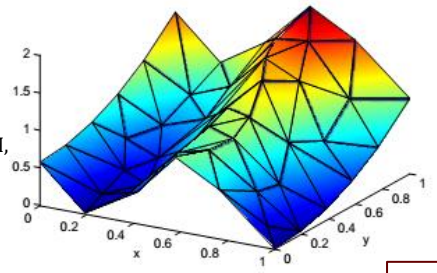

Traditional mesh-based methods FDM, FVM, FEM

Implement and execute it on different computer architectures

```
class trivial2D : public optimObjBase{
      typedef trivial2D TT;
public:
      ///PARAMETERs AND CRITERIA definition
      enum CriteriaName{R1,endCrit};
      enum ParamName{X,Y,endParam};
      trivial2D(){
            params.resize(endParam);
            criteria.resize(endCrit);
      }
};
```

Final goal is to create expressive, robust and computationally efficient implementation of numerical solution procedure

Differential operator approximation

The main idea behind meshless method is the approximation of differential operators over the local cluster of nodes, in many cases simply *n* closest nodes

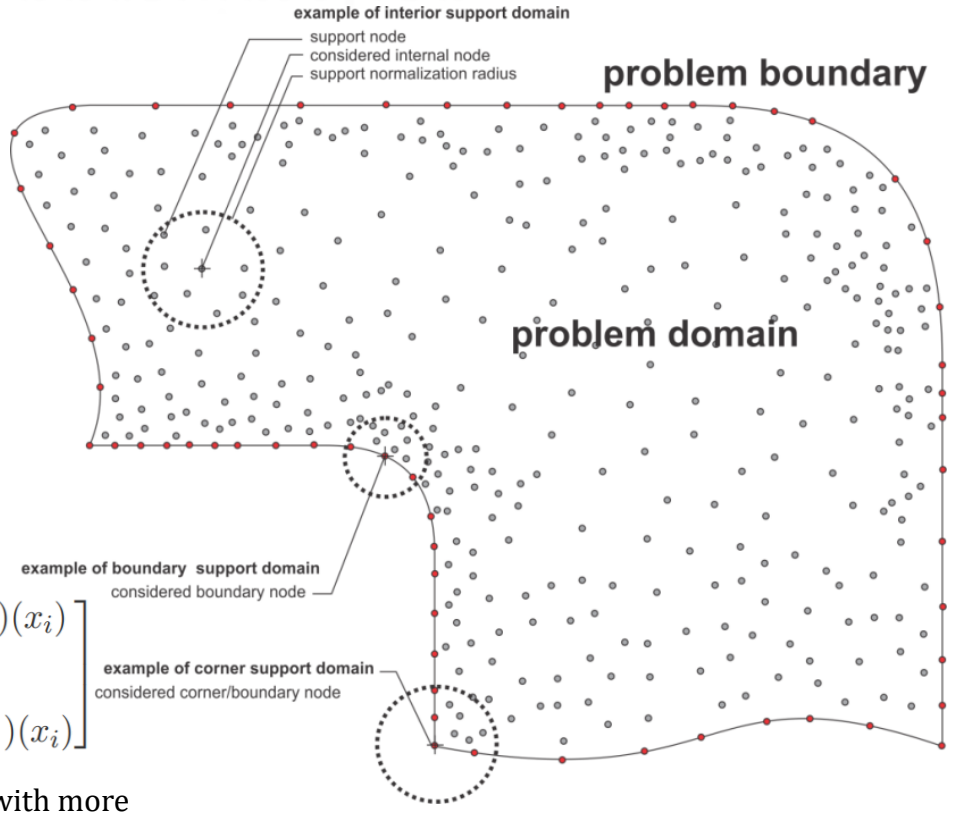

Differential operator is approximated as

$$(\mathcal{L}u)(x_i) \approx \sum_{x_j \in N(x_i)} w_j^i u(x_j)$$

Imposing exactness for a certain set of basis functions, e.g. monomials, MQs, Gaussians, etc., results in a system

$$\begin{bmatrix} \varphi(\|x_{j_1} - x_{j_1}\|) & \cdots & \varphi(\|x_{j_{n_i}} - x_{j_1}\|) \\ \vdots & \ddots & \vdots \\ \varphi(\|x_{j_1} - x_{j_{n_i}}\|) & \cdots & \varphi(\|x_{j_{n_i}} - x_{j_{n_i}}\|) \end{bmatrix} \begin{bmatrix} w_{j_1}^i \\ \vdots \\ w_{j_{n_i}}^i \end{bmatrix} = \begin{bmatrix} (\mathcal{L}\varphi_{j_1})(x_i) \\ \vdots \\ (\mathcal{L}\varphi_{j_{n_i}})(x_i) \end{bmatrix}$$

That can be subjected to additional weighting (W), when working with more nodes in support than basis functions (n>m) [1]

To enforce consistency of the approximation system can be augmented with monomials up to a certain order

$$\begin{bmatrix} A & P \\ P^{\mathsf{T}} & 0 \end{bmatrix} \begin{bmatrix} \boldsymbol{w} \\ \boldsymbol{\lambda} \end{bmatrix} = \begin{bmatrix} \boldsymbol{\ell}_\varphi \\ \boldsymbol{\ell}_p \end{bmatrix} \qquad P = \begin{bmatrix} p_1(\boldsymbol{x}_1) & \cdots & p_s(\boldsymbol{x}_1) \\ \vdots & \ddots & \vdots \\ p_1(\boldsymbol{x}_n) & \cdots & p_s(\boldsymbol{x}_n) \end{bmatrix}, \quad \boldsymbol{\ell}_p = \begin{bmatrix} (\mathcal{L}p_1)|_{\boldsymbol{x}=\boldsymbol{x}^*} \\ \vdots \\ (\mathcal{L}p_s)|_{\boldsymbol{x}=\boldsymbol{x}^*} \end{bmatrix}$$

[1] http://e6.ijs.si/medusa/wiki/index.php/Computation_of_shape_functions

Differential operator approximation

Several strong form methods that can be described with this approach

Finite Differences Method → n=3, W(p)=1, b={1, x, x2} on regular nodes

Local Radial Basis Function Collocation Method → n, W(p)=1, b={sqrt(1+(p/c)2)}, m=n
Šarler, B. (2007): From global to local radial basis function collocation method for transport phenomena, Advances in Meshfree Techniques, Springer, Berlin, pp. 257-282.

Finite pointset method → n=20-50, W(p)=exp(-(p/s)2), b={1, x, x^2, …}
S Tiwari, J Kuhnert - Meshfree methods for partial differential equations, 2003 - Springer

Diffuse Approximate Method → n=13, W(p)=exp(-(p/s)2), b ={1, x, y, x^2, y^2, xy}
Diffuse approximation method for solving natural convection in porous media,C Prax, H Sadat, P Salagnac - Transport in Porous Media, 1996 – Springer

Radial basis function generated finite differences (RBF-FD) → n=12, basis = r^3, augmentation ={1, x, y, x^2, y^2, xy}
Accuracy of radial basis function interpolation and derivative approximations on 1-D infinite grids, B Fornberg, N. Flyer - Advances in Computational Mathematics, 2005 – Springer

… and many more

More details on differential operator approximation such as complexity analysis, ghost nodes, boundary conditions, implementation notes, stability, … can be found at out discussion wiki page -- http://e6.ijs.si/medusa/wiki/index.php/Medusa

Discretization of the domain

It is generally accepted that quasi-uniformly-spaced node sets improve the stability of meshless methods

Holger Wendland. Scattered data approximation. Number 17 in Cambridge Monographs on Applied and Computational Mathematics. Cambridge University Press, 2004

The most basic way to generate node sets is to employ existing tools and algorithms for mesh generation, use the generated nodes and simply discard the connectivity relations

(G.-R. Liu, Mesh free methods: moving beyond the finite element method, CRC press, 2002)

- Conceptually flawed
- Expensive
- Inappropriate for meshless

A common iterative approach is to position nodes by simulating free charged particles, obtaining so-called minimal energy nodes, Other iterative methods include bubble simulation, Voronoi relaxation or a combination of both. [17, 24, 1]

(D. P. Hardin and E. B. Saff, Discretizing manifolds via minimum energy points, Notices of the AMS, 51 (2004), pp. 1186-1194

Y. Liu, Y. Nie, W. Zhang, and L. Wang, Node placement method by bubble simulation and its application, Computer Modeling in Engineering and Sciences(CMES), 55 (2010), p. 89)

- Iterative methods are computationally expensive and require an initial distribution
- can be used as a post processing

Advancing front methods, which usually begin at the boundary and advance towards the domain interior, filling it in the process.

(R. Lohner and E. Onate , A general advancing front technique for filling space with arbitrary objects, Int. J. Numer. Methods Eng., 61 (2004), pp. 1977)

- Often limited to 2D

Circle or sphere packing methods

(X.-Y. Li, S.-H. Teng, and A. Ungor, Point placement for meshless methods using sphere packing and advancing front methods, in ICCES'00, Los Angeles, CA, Citeseer, 2000.)

- Expensive
- Good quality of nodal distribution

Poisson Disk sampling based algorithms (also advancing front type node generation)

(R. L. Cook, Stochastic sampling in computer graphics, ACM Trans. Graphics, 5 (1986), pp. 51

V. Shankar, R. M. Kirby, and A. L. Fogelson, Robust node generation for meshfree discretizations on irregular domains and surfaces, SIAM J. Sci. Comput., 40 (2018), pp. 2584

Slak J., Kosec G., On Generation of Node Distributions for Meshless PDE Discretizations, SIAM Journal on Scientific Computing, 41(5))

- Computationally effective
- Dimension independent
- Good quality of nodal distribution

Meshless node generation

Dimension independent Poisson disc sampling based node generation algorithm supporting spatially variable density distribution

- Local regularity with minimal spacing guaranteed
- Spatially variable density
- Scalable
- Compatible with irregular domains
- Dimension independent

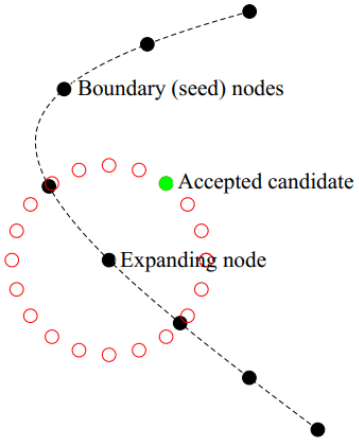

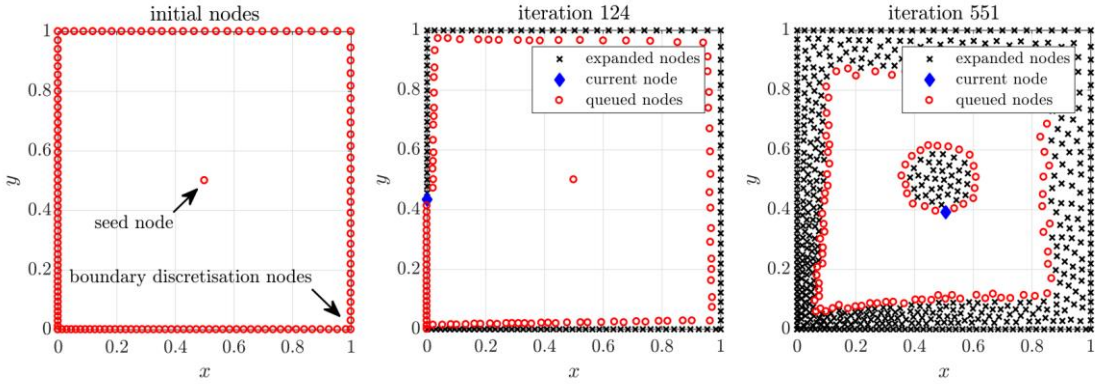

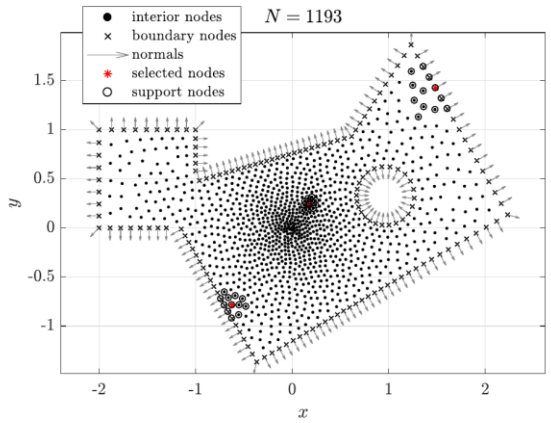

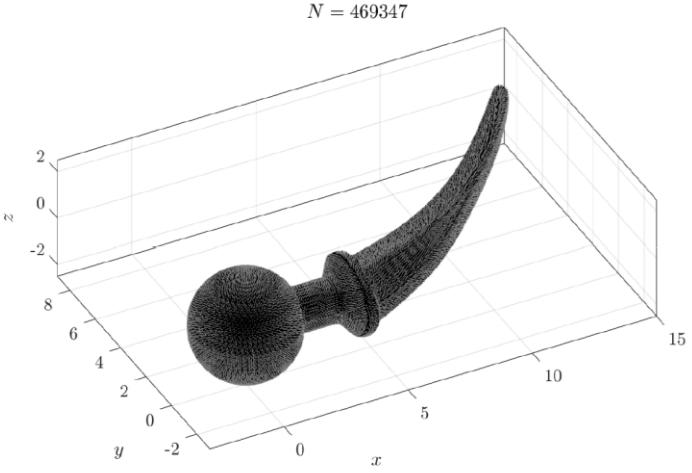

$$x_1 = r\cos(\phi_1)$$
$$x_2 = r\sin(\phi_1)\cos(\phi_2)$$
$$x_3 = r\sin(\phi_1)\sin(\phi_2)\cos(\phi_3)$$
$$\vdots$$
$$x_{d-1} = r\sin(\phi_1)\cdots\sin(\phi_{d-2})\cos(\phi_{d-1})$$
$$x_d = r\sin(\phi_1)\cdots\sin(\phi_{d-2})\sin(\phi_{d-1})$$

Extension to parametric surfaces and CAD geometry

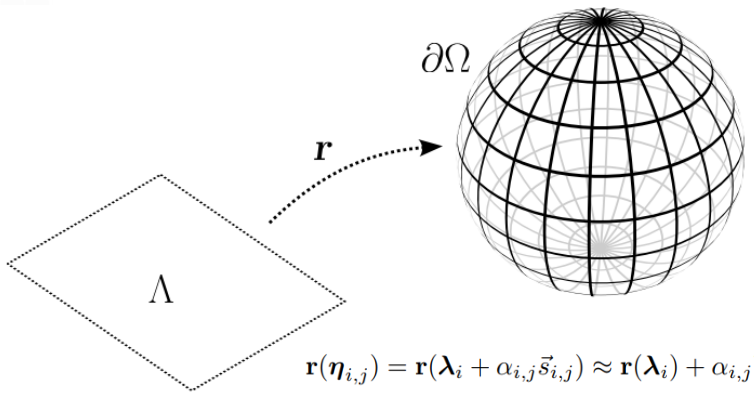

$$\mathbf{r}(\boldsymbol{\eta}_{i,j}) = \mathbf{r}(\boldsymbol{\lambda}_i + \alpha_{i,j}\vec{s}_{i,j}) \approx \mathbf{r}(\boldsymbol{\lambda}_i) + \alpha_{i,j}\nabla\mathbf{r}(\boldsymbol{\lambda}_i)\vec{s}_{i,j}.$$

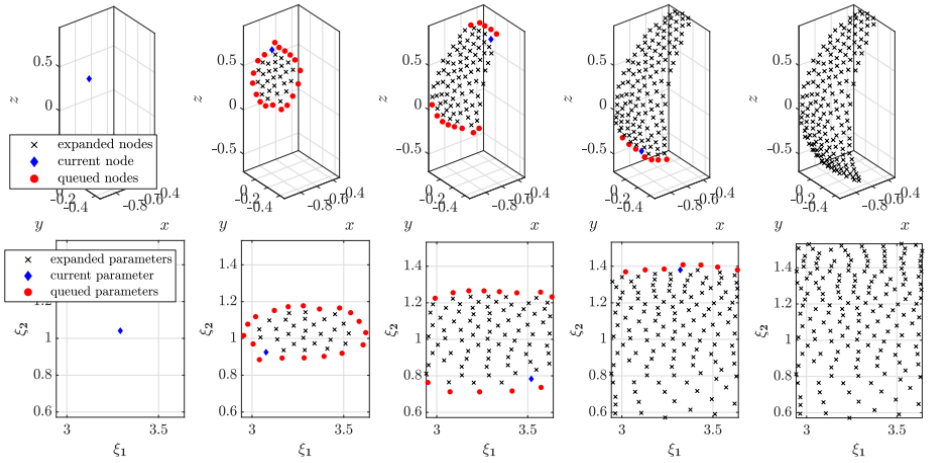

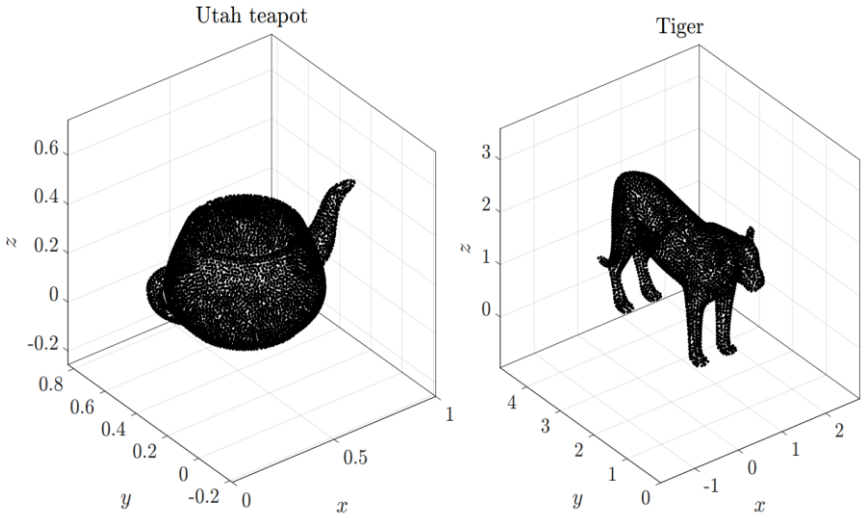

Node sets generated by NURBS-DIVG on a CAD Utah Teapot (left) and a CAD model of tiger (right). The Utah Teapot model is made of 32 patches and has 7031 nodes; the tiger has 124 patches and 4753 boundary nodes.

CAD models typically consist of multiple non-overlapping and abutting NURBS surface patches. A NURBS patch meets another NURBS patch at a NURBS curve (the boundary curves of the respective patches)

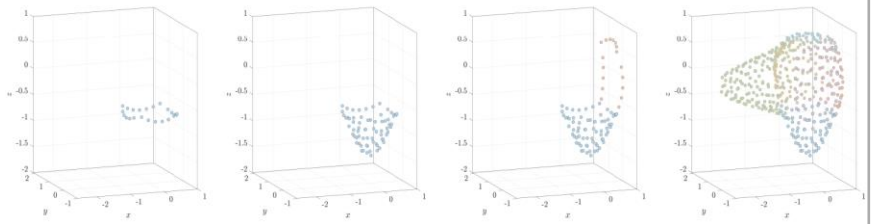

Adaptivity

We can change the order of the method by varying order of augmenting monomials (p-adaptivity/refinement)

- Higher order method requires bigger stencil -- $n = 2\binom{m+d}{d}$

m	$d = 1$	$d = 2$	$d = 3$
2	6	12	20
4	10	30	70
6	14	56	168
8	18	90	330

We can control local internodal distance via density function in DIVG node positioning algorithm (h-adaptivity/refinement)

- h – adaptivity/refinement is inherently included in the meshless methods

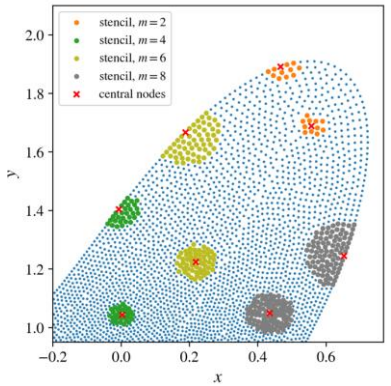

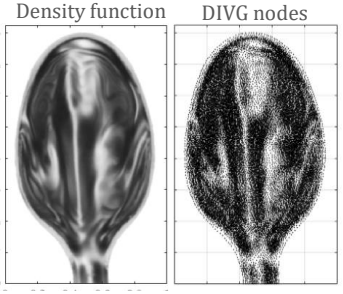

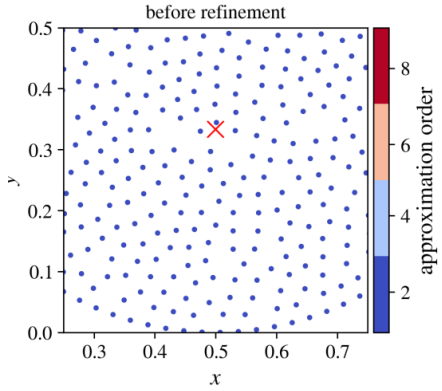

Adaptive solution procedure

- Solve governing PDE with given node and order distribution.
- Estimate error
- Mark nodes for refinement/de-refinement
- Recompute with new setup
- repeat

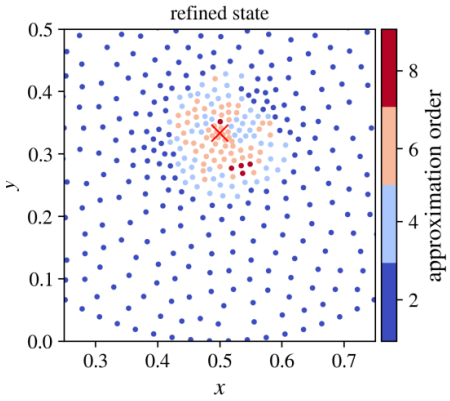

The modified Texas Three-Fold marking strategy

Each node is tested for refinement action based on error indicator
(or actual error or any other quantity we would like to consider)

$$\begin{cases} \eta_i > \alpha\eta_{max}, & \text{refine} \\ \beta\eta_{max} \le \eta_i \le \alpha\eta_{max}, & \text{do nothing} \\ \eta_i < \beta\eta_{max}, & \text{derefine} \end{cases}$$

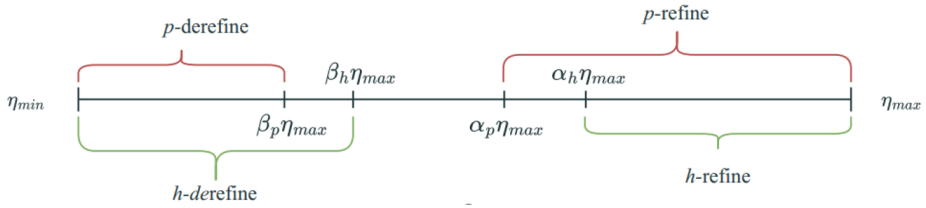

η_i

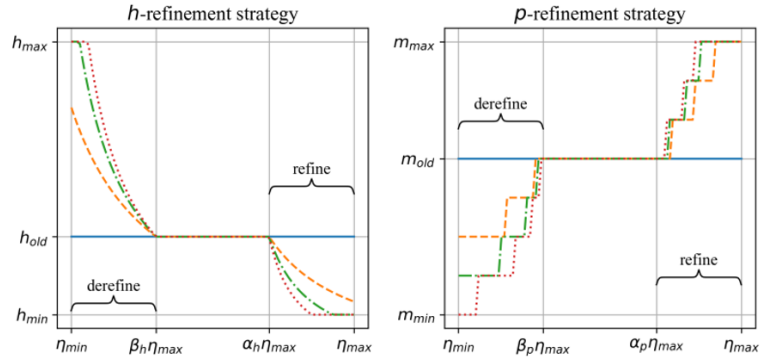

Example of 4 step *h*-refinement of a simple test function approximation with nodal density increase factor *f*

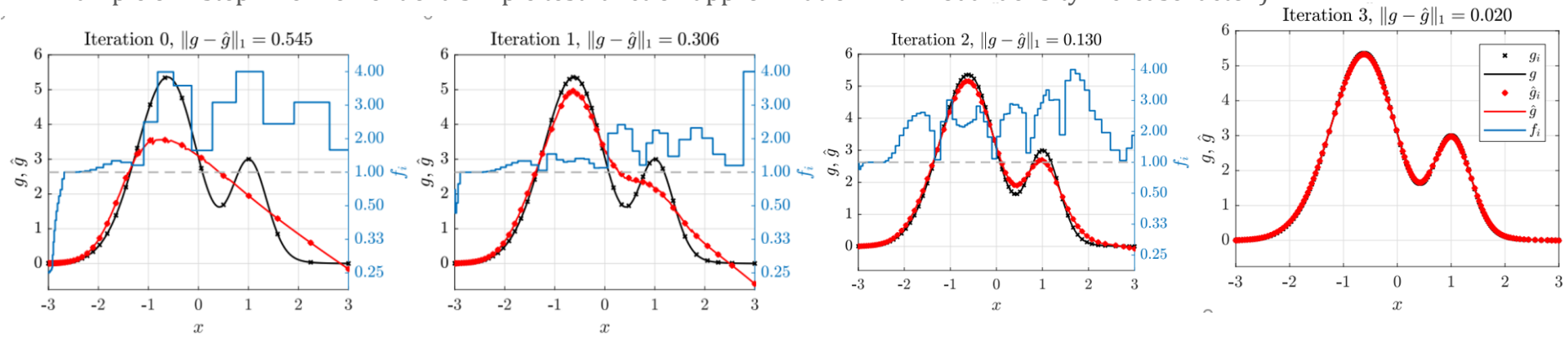

$g(x) = 3(1-x)^2\exp(-x^2) + 3\exp(-4(x-1)^2)$ Test function

IMEX Error indicator

Consider a problem of type

$$\mathcal{L}u = f_{RHS}.$$

The IMplicit-EXplicit error indicator:

1. Obtain implicit solution $u^{(im)}$ to governing problem using low-order approximations of $\mathcal{L}$, i.e. $\mathcal{L}^{(lo)}_{(im)}$.
2. Obtain high-order approximations o explicit operators $\mathcal{L}$, i.e. $\mathcal{L}^{(hi)}_{(ex)}$
3. Apply $\mathcal{L}^{(hi)}_{(ex)}$ to $u^{(im)}$ and obtain $f_{(ex)}$ the process
4. Compare f_{RHS} and $f_{(ex)}$

$$\begin{aligned}
\nabla^2 u(\boldsymbol{x}) &= 2ae^{-a\|\boldsymbol{x}-\boldsymbol{x}_s\|^2}(2a\,\|\boldsymbol{x}-\boldsymbol{x}_s\| - d) && \text{in } \Omega,\\
u(\boldsymbol{x}) &= e^{-a\|\boldsymbol{x}-\boldsymbol{x}_s\|^2} && \text{on } \Gamma_d,\\
\nabla u(\boldsymbol{x}) &= -2a(\boldsymbol{x}-\boldsymbol{x}_s)e^{-a\|\boldsymbol{x}-\boldsymbol{x}_s\|^2} && \text{on } \Gamma_n,
\end{aligned}$$

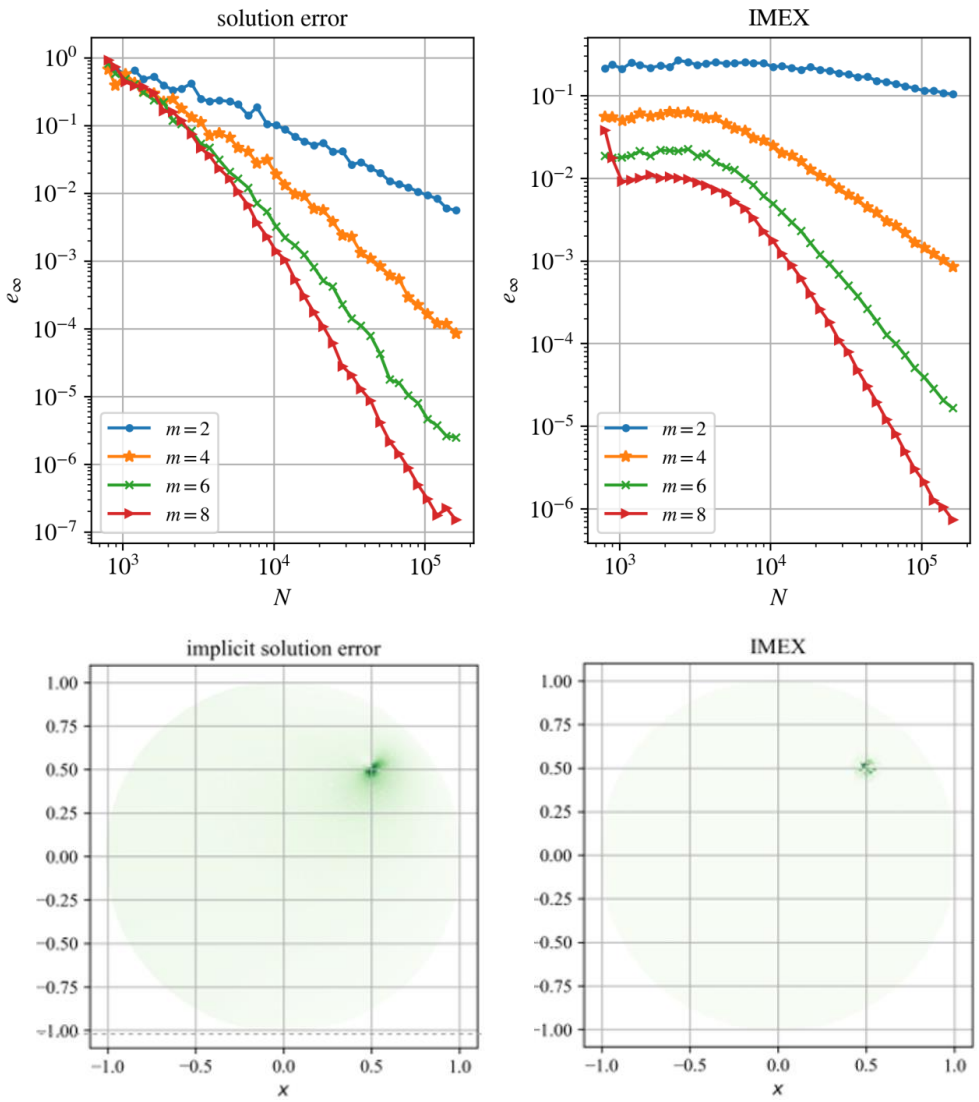

High order solution of Poisson's problem

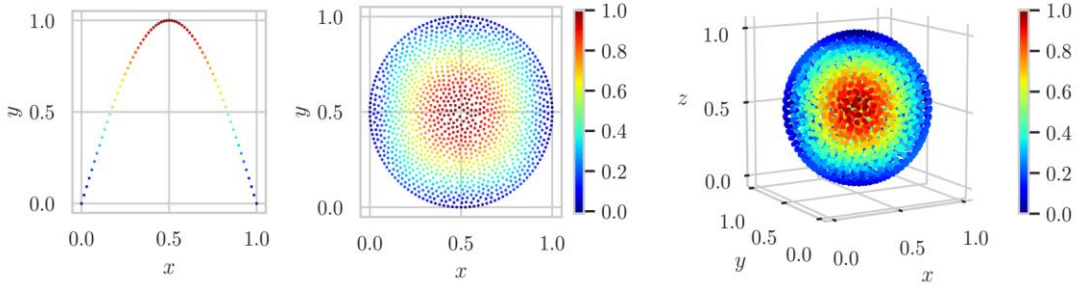

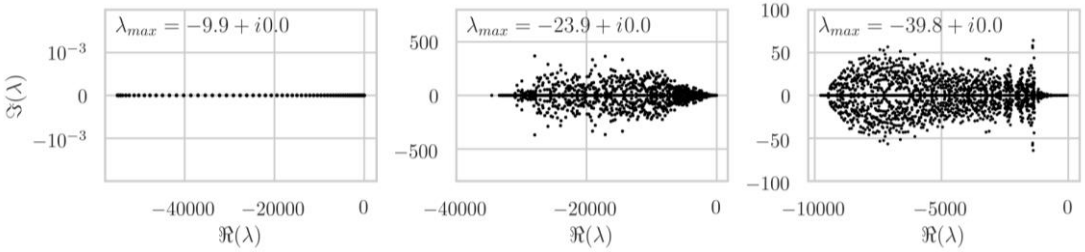

$$\nabla^2 u(\boldsymbol{x}) = -d\pi^2 \prod_{i=1}^{d} \sin(\pi x_i)$$

$$u(\boldsymbol{x}) = \prod_{i=1}^{d} \sin(\pi x_i)$$

$$\frac{\partial u}{\partial \boldsymbol{n}}(\boldsymbol{x}) = \pi \sum_{i=1}^{d} n_i \cos(\pi x_i) \prod_{j \neq i} \sin(\pi x_j)$$

$$\Omega = \left\{ \boldsymbol{x},\ \left\| \boldsymbol{x} - \frac{\mathbf{1}}{\mathbf{2}} \right\| < \frac{1}{2} \right\},$$

$$\Gamma_d = \left\{ \boldsymbol{x} \in \partial\Omega,\ x_1 < \frac{1}{2} \right\},$$

$$\Gamma_n = \left\{ \boldsymbol{x} \in \partial\Omega,\ x_1 \geq \frac{1}{2} \right\}.$$

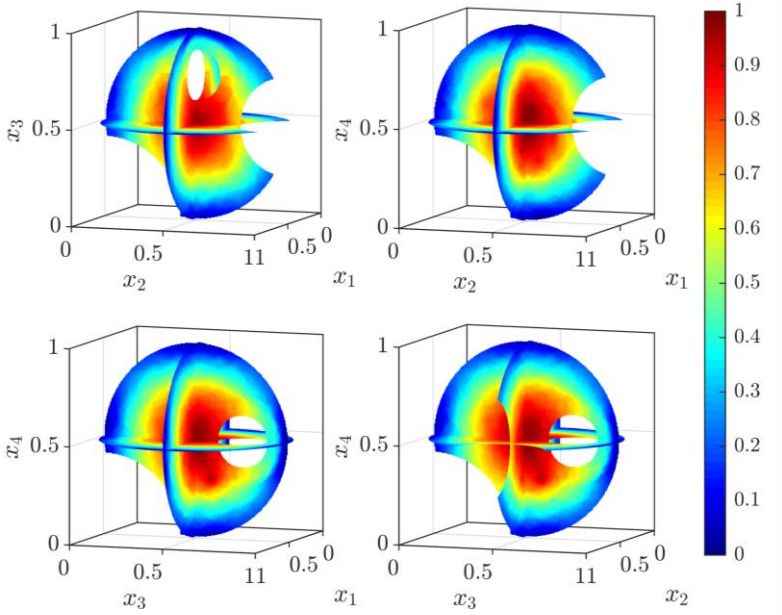

3-dimensional cross sections of a solution to 4-dimensional Poisson problem

Adaptive solution of Poisson's problem

Poisson problem with exponentially strong source in the domain

$$\nabla^2 u(\boldsymbol{x}) = 2ae^{-a\|\boldsymbol{x}-\boldsymbol{x}_s\|^2}(2a\,\|\boldsymbol{x}-\boldsymbol{x}_s\| - d) \quad \text{in } \Omega,$$
$$u(\boldsymbol{x}) = e^{-a\|\boldsymbol{x}-\boldsymbol{x}_s\|^2} \quad \text{on } \Gamma_d,$$
$$\nabla u(\boldsymbol{x}) = -2a(\boldsymbol{x}-\boldsymbol{x}_s)e^{-a\|\boldsymbol{x}-\boldsymbol{x}_s\|^2} \quad \text{on } \Gamma_n$$

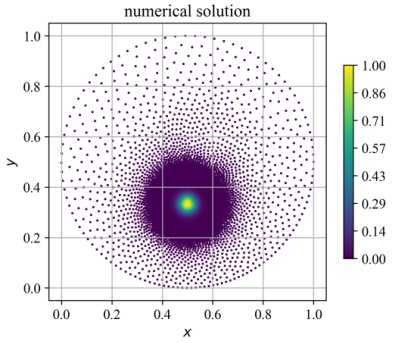

Setup

- RBF-FD
- PHS order $k = 3$
- Monomial augmentation with $m \in \{2, 4, 6, 8\}$
- IMEX with monomials $m \in \{4, 6, 8, 10\}$

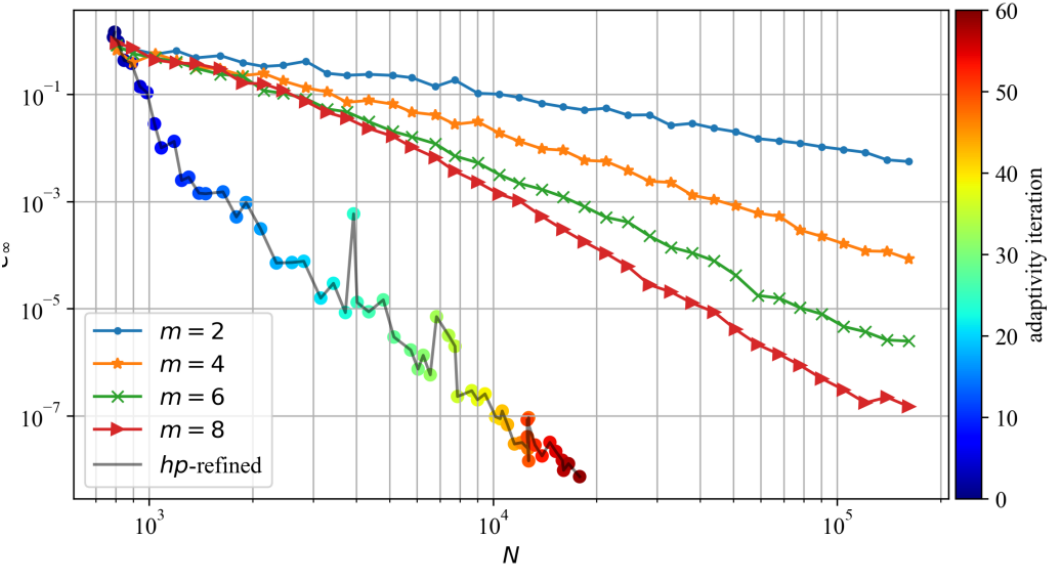

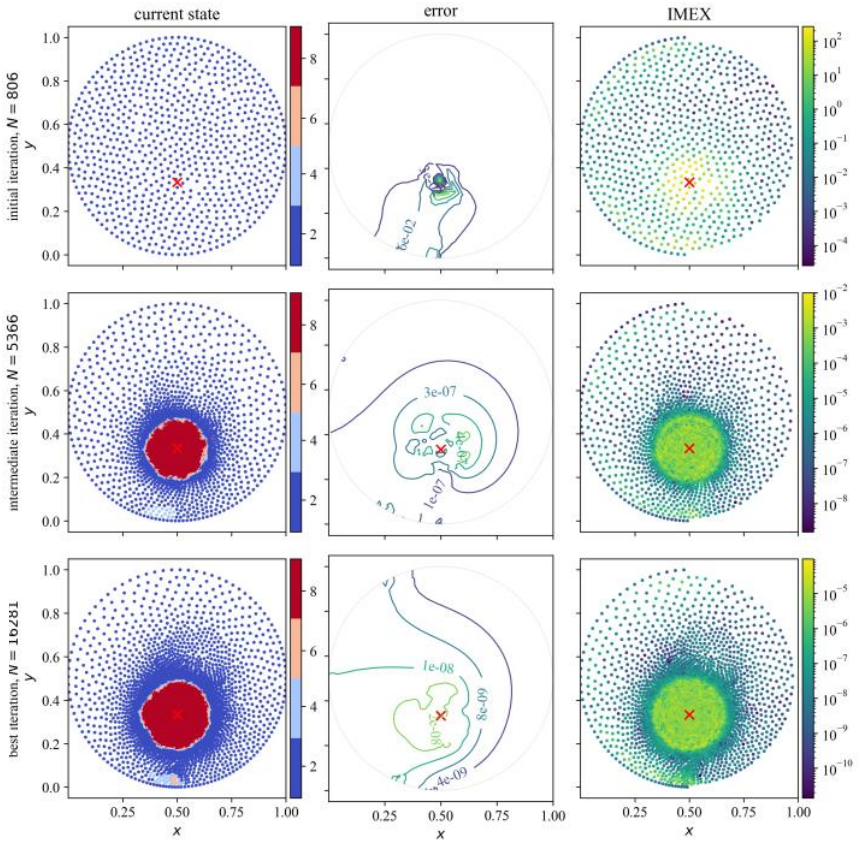

Adaptive fretting fatigue simulation

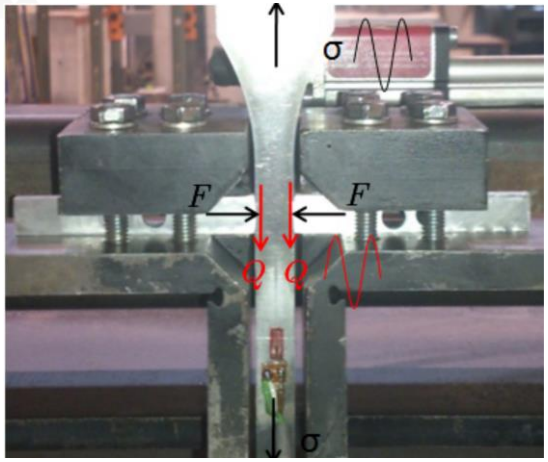

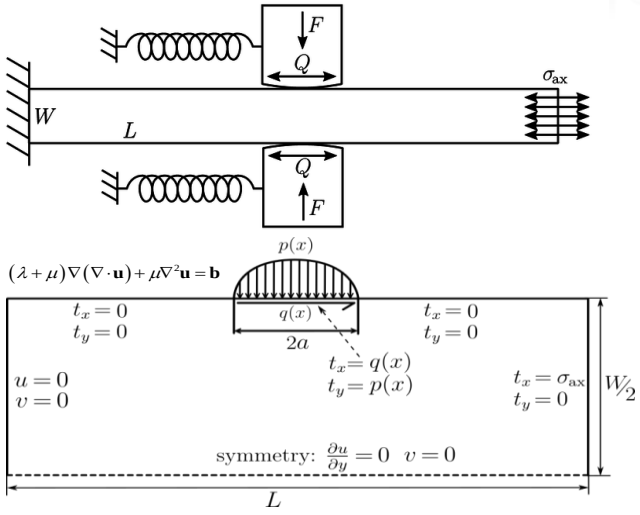

- Research Foundation – Flanders – (FWO)

fwo Opening new horizons

- The Luxembourg National Research Fund (FNR)

Luxembourg National Research Fund

- Slovenian Research Agency (ARRS)

Slovenian Research Agency

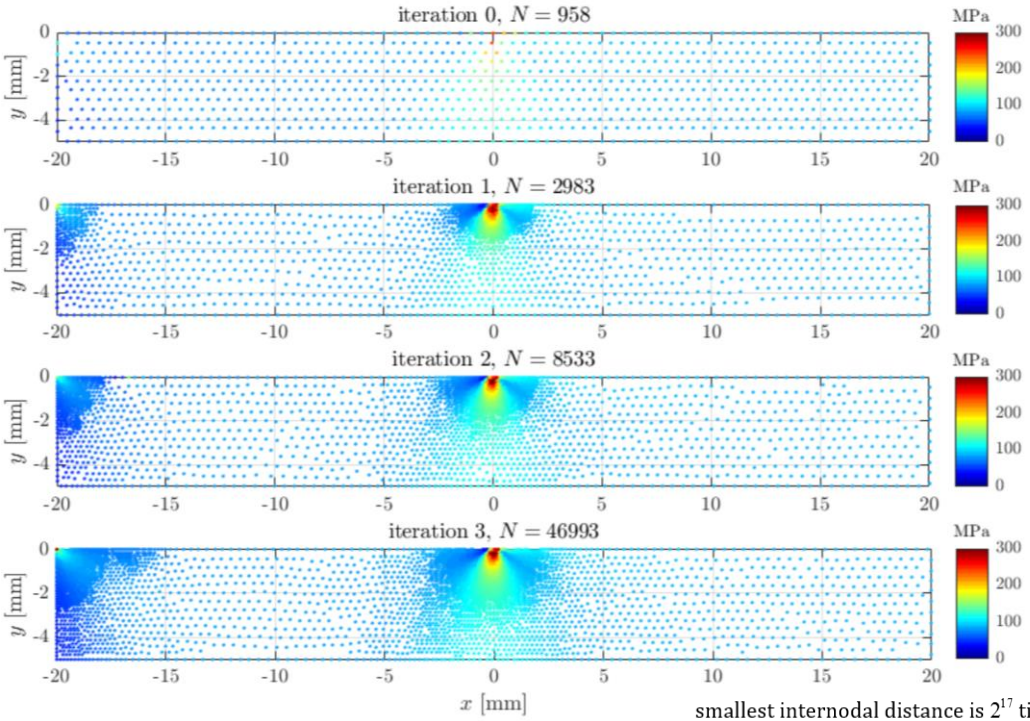

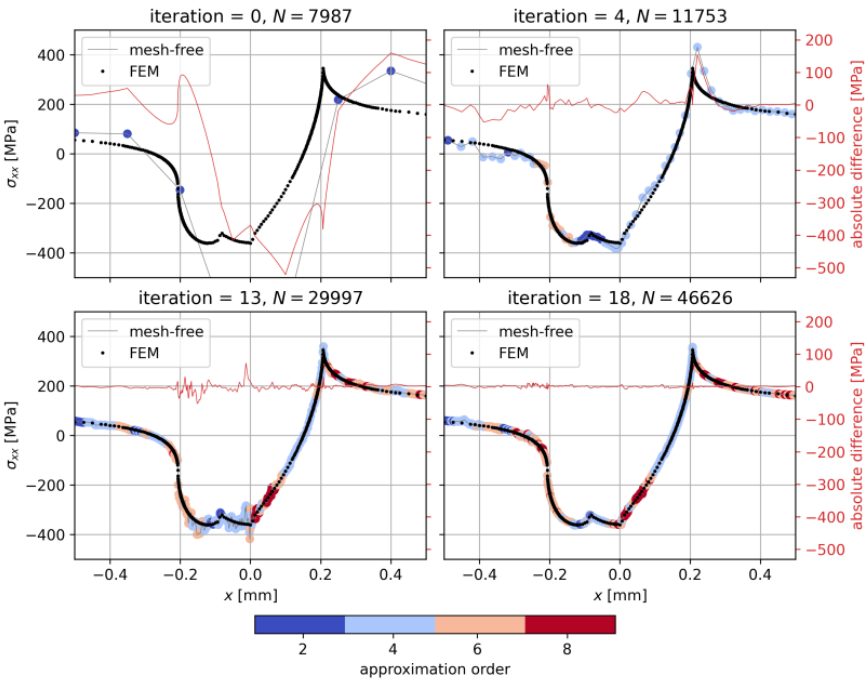

smallest internodal distance is 2^{17} times smaller than the initial one

Consideration of irregular 3D domains

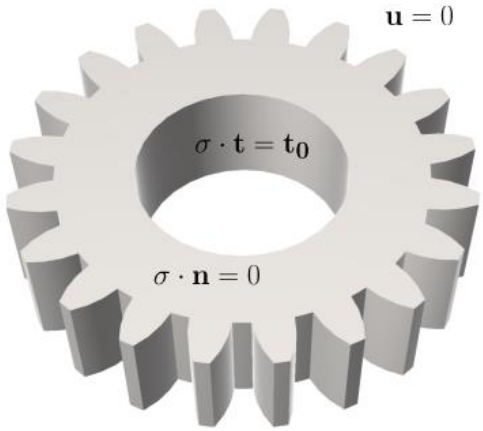

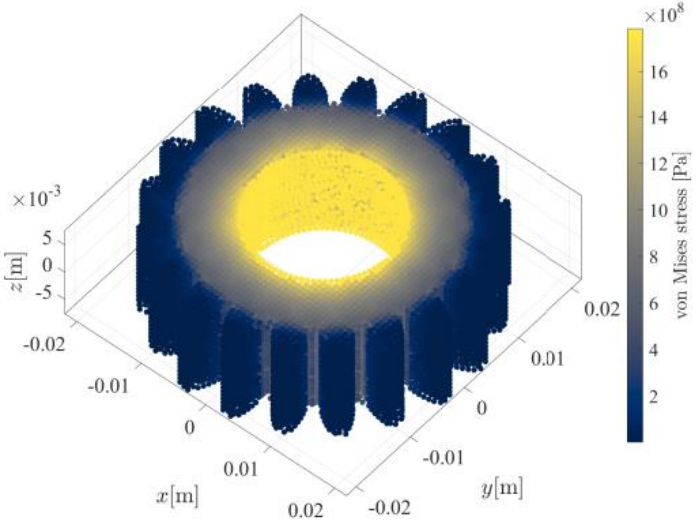

Elastic deformation of a 3D gear object that is subjected to the external torque resulting in the tangential traction on axis, while the gear teeth are blocked.

$$\frac{E}{2(\nu+1)}\left(\nabla^2\mathbf{u} + \frac{1}{1-2\nu}\nabla(\nabla\cdot\mathbf{u})\right) = 0$$
$$\mathbf{u} = 0, \quad \text{on } \Gamma_{\text{teeth}},$$
$$\sigma\cdot\mathbf{n} = 0, \quad \text{on } \Gamma_{\text{free}},$$
$$\sigma\cdot\mathbf{t} = t_0\mathbf{t}, \quad \text{on } \Gamma_{\text{axis}}.$$

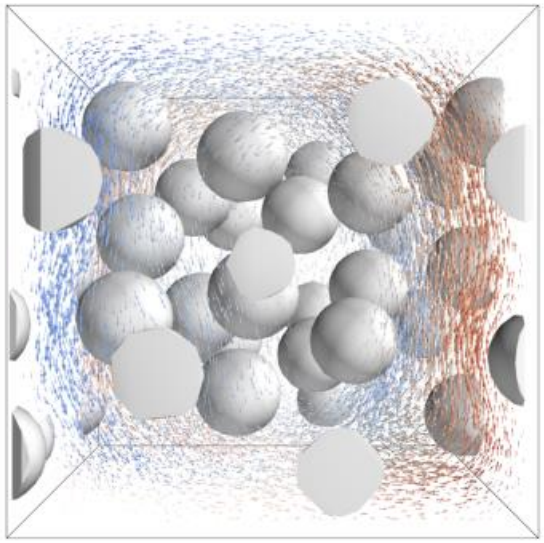

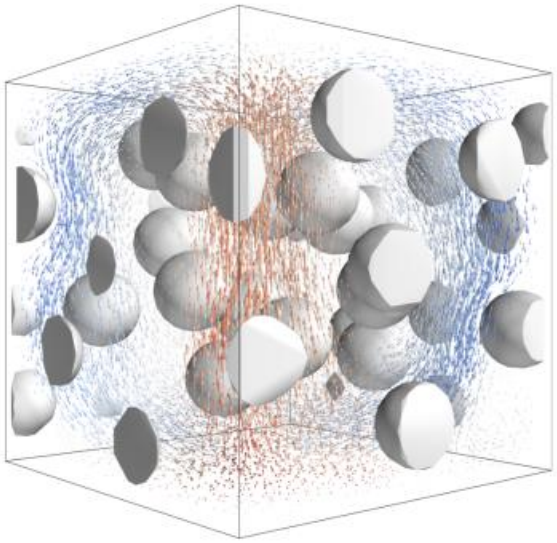

Non-Newtonian natural convection in randomly generated domain with differentially heated vertical walls and isolated horizontal walls

$$\nabla\cdot\boldsymbol{v} = 0,$$
$$\rho\left(\frac{\partial\boldsymbol{v}}{\partial t} + \boldsymbol{v}\cdot\nabla\boldsymbol{v}\right) = -\nabla p + \nabla\cdot(\eta\nabla\boldsymbol{v}) - \boldsymbol{g}\rho\beta T_\Delta,$$
$$\rho c_p\left(\frac{\partial T}{\partial t} + \boldsymbol{v}\cdot\nabla T\right) = \nabla\cdot(\lambda\nabla T),$$
$$\eta = \eta_0\left(\frac{1}{2}\left\|\nabla\boldsymbol{v} + (\nabla\boldsymbol{v})^T\right\|\right)^{\frac{n-1}{2}},$$

Moving boundary problems

Meshless interface tracking for the simulation of dendrite envelope growth including surface reconstruction and h-adaptive cloud points.

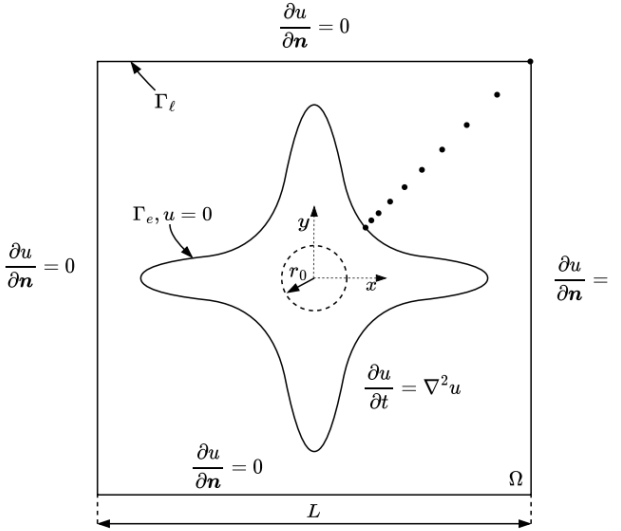

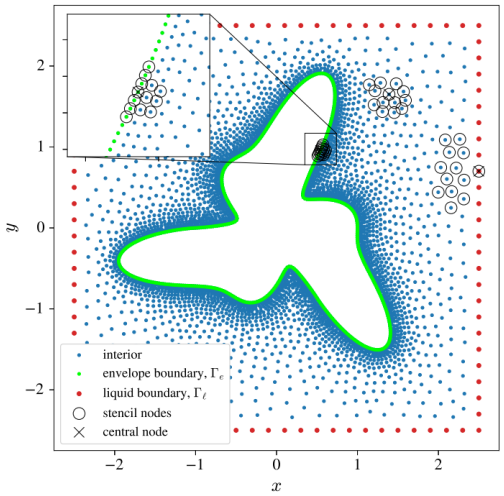

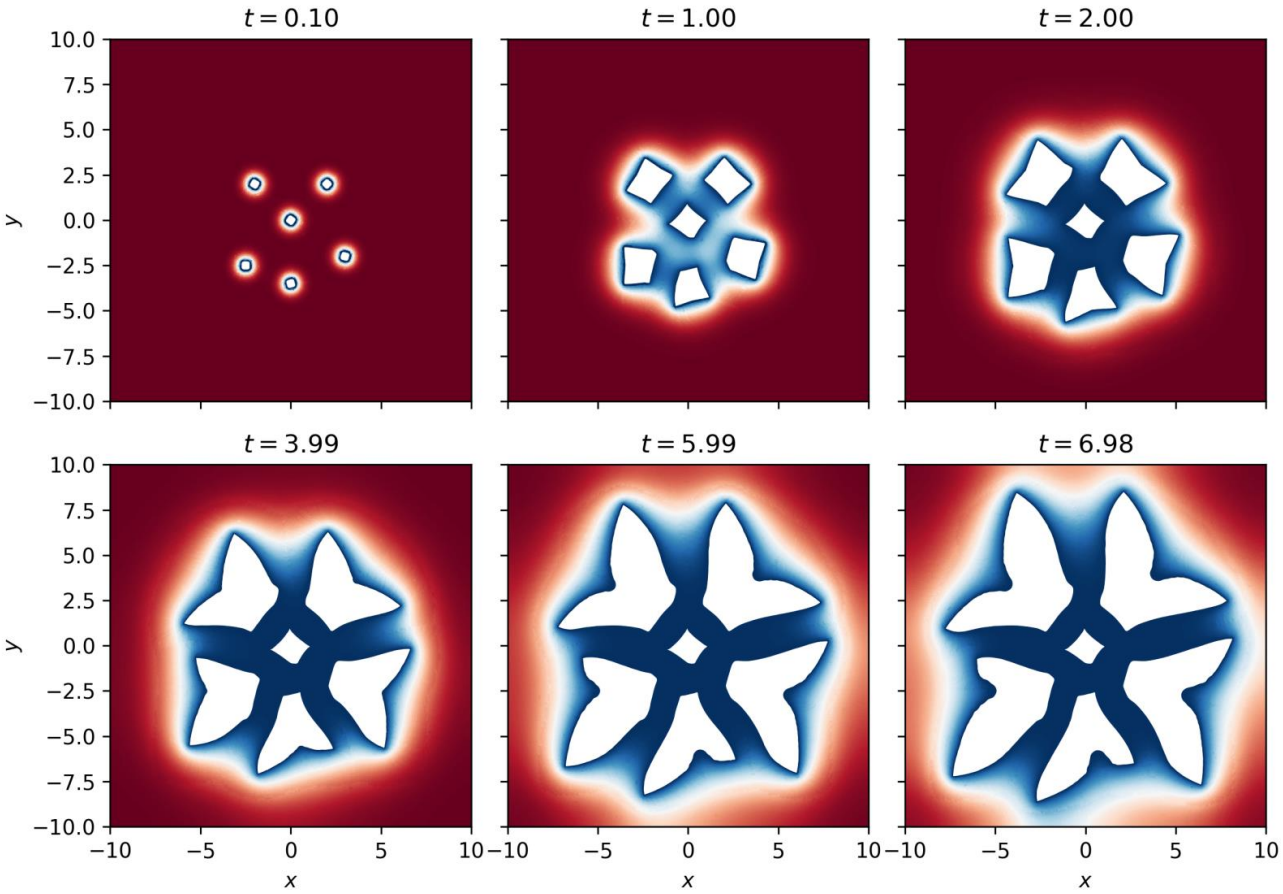

Growth of six interacting dendrites with different orientations of the tip growth directions.

Solidification of a binary alloy

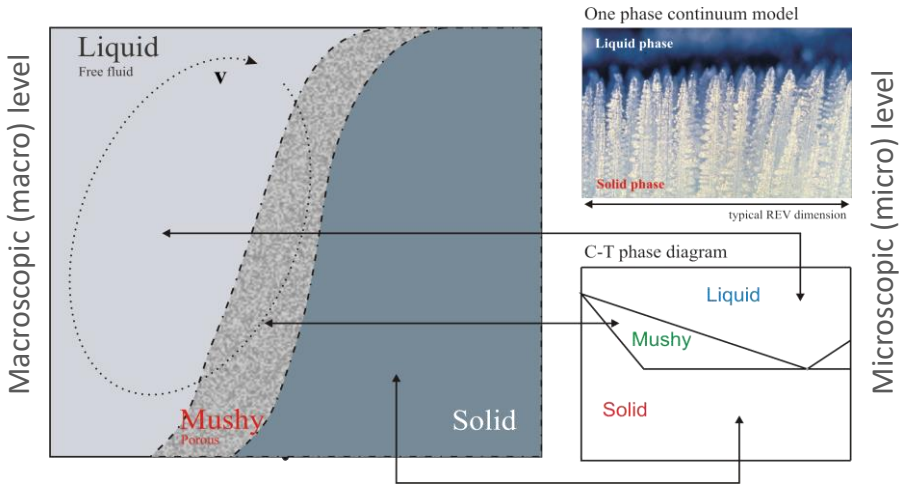

Governing PDEs

$$\langle \mathbf{v} \rangle = f_L \mathbf{v}_L$$

$$\nabla \cdot \langle \mathbf{v} \rangle = 0$$

$$\rho \frac{\partial \langle \mathbf{v} \rangle}{\partial t} + \frac{\rho}{f_L} \nabla \cdot \left(\langle \mathbf{v} \rangle \langle \mathbf{v} \rangle \right) = - f_L \nabla P + \nabla \cdot \left(\mu \nabla \langle \mathbf{v} \rangle \right) - f_L \frac{\mu}{K} \langle \mathbf{v} \rangle + f_L \mathbf{b}$$

$$\rho \frac{\partial \langle h \rangle}{\partial t} + \rho \langle \mathbf{v} \rangle \cdot \nabla \langle h \rangle = \nabla \cdot \left(\lambda \nabla T \right)$$

$$\frac{\partial \langle C \rangle}{\partial t} + \langle \mathbf{v} \rangle \cdot \nabla C_L = 0$$

Adaptive upwind

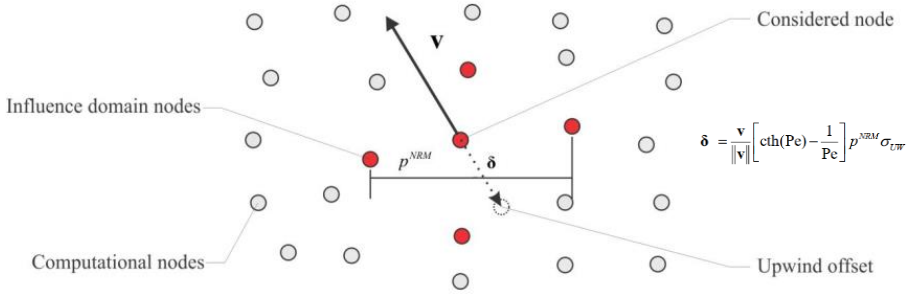

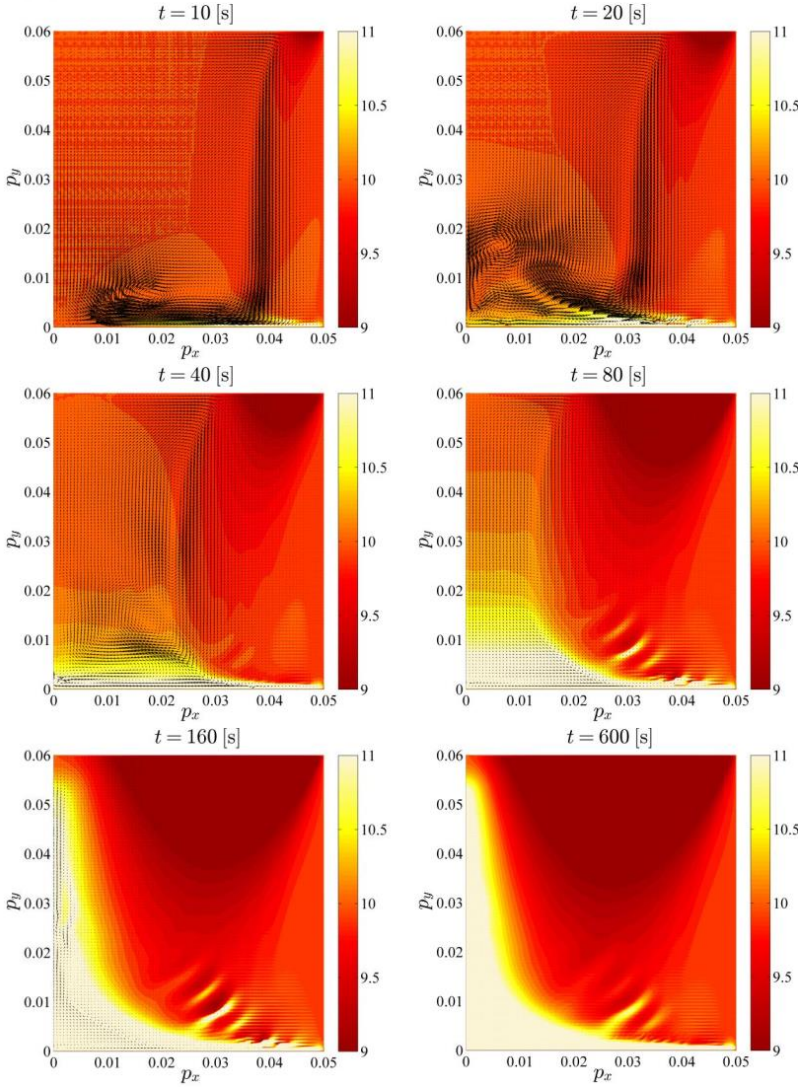

Concentration and velocity at different stages of Sn-10%Pb alloy solidification. Last (bottom right) plot stands for fully solidified state.

Small-strain elasto-plastic deformation

Internally Pressurized Thick-Walled Cylinder

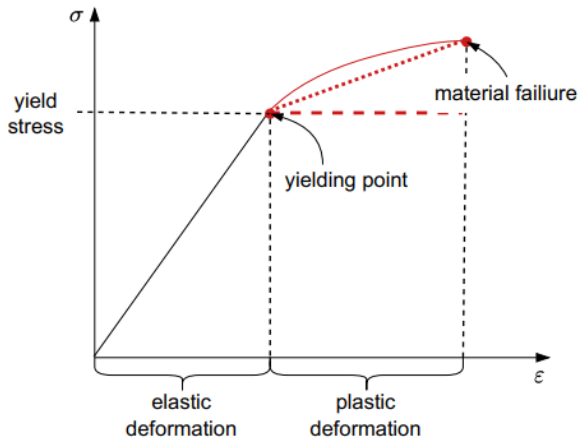

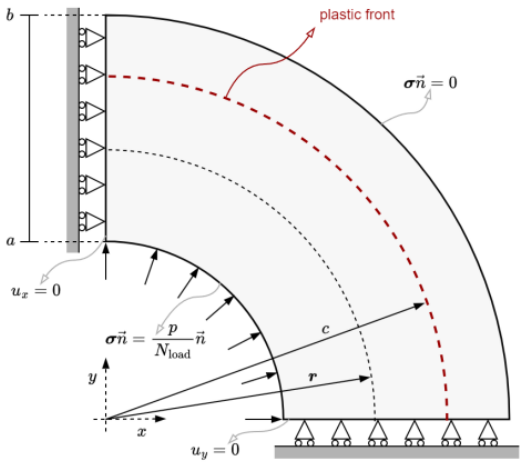

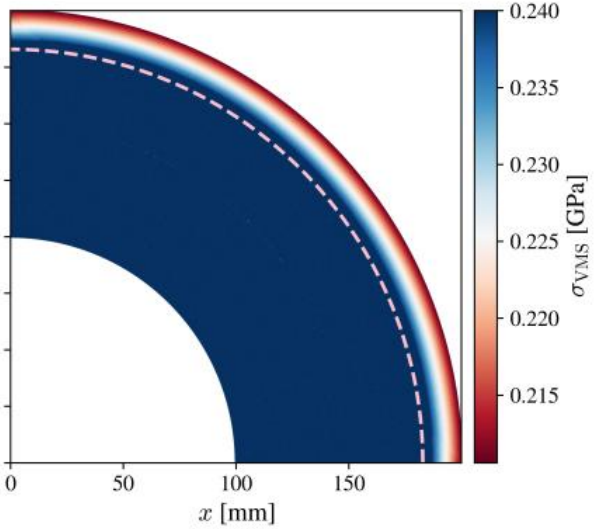

Elastic regime – Navier Cauchy problem

$$(\lambda + \mu)\,\nabla(\nabla \cdot \vec{u}) + \mu\nabla^2\vec{u} = 0$$

Upon surpassing a critical stress threshold the material experiences localized irreversible plastic deformation – von Mises criterion

$$\begin{cases} \Phi \leq 0, & \text{(elastic deformation), solution is locally valid} \\ \Phi > 0, & \text{(plastic deformation), solution is locally invalid} \end{cases}$$

$$\Phi = \sigma_{\text{VMS}n} - \sigma_y(\bar{\varepsilon}_n^p)$$

plastic regime a correction

$$\vec{u}_i = \vec{u}_{i-1} + \delta\vec{u}$$

$$\delta\boldsymbol{\varepsilon} = \frac{\nabla(\delta\vec{u}) + (\nabla(\delta\vec{u}))^{\intercal}}{2}$$

$$\boldsymbol{\varepsilon}_i^{\text{e}} = \boldsymbol{\varepsilon}_{i-1}^{\text{e}} + \delta\boldsymbol{\varepsilon}$$

$$\boldsymbol{\varepsilon}_i^{p} = \boldsymbol{\varepsilon}_{i-1}^{p}$$

$$\bar{\varepsilon}_i^{p} = \bar{\varepsilon}_{i-1}^{p}$$

$$\boldsymbol{\sigma}_i = \mathbf{D}^{\text{e}}\boldsymbol{\varepsilon}_i^{\text{e}}$$

Return mapping algorithm

$$\Phi = \sigma_{\text{VMS}i} - 3\mu\Delta\gamma - \sigma_y(\bar{\varepsilon}_i^p + \Delta\gamma) = 0$$

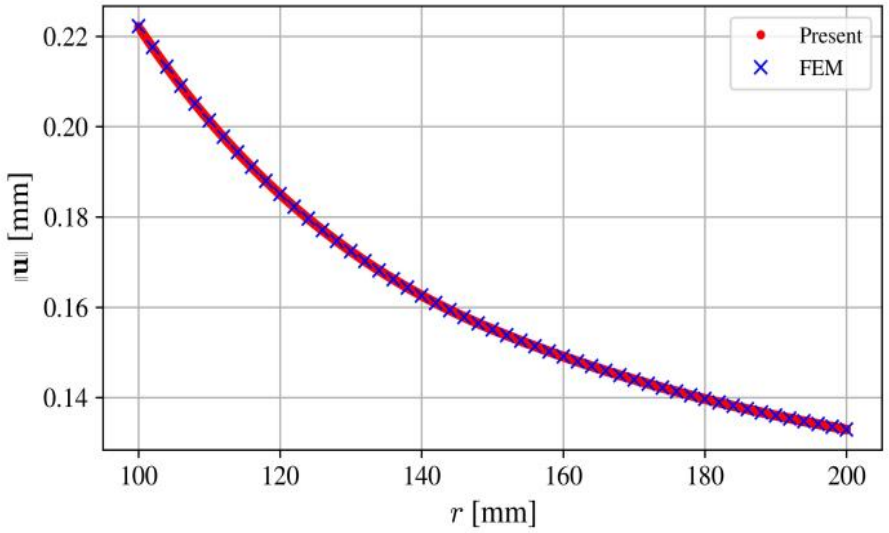

Displacement magnitude vs radial coordinate – comparison of pure RBF-FD solution with ABAQUS solution

Inertial effects on fluid flow in complex porous media

Body force driven Flow through periodic lattice

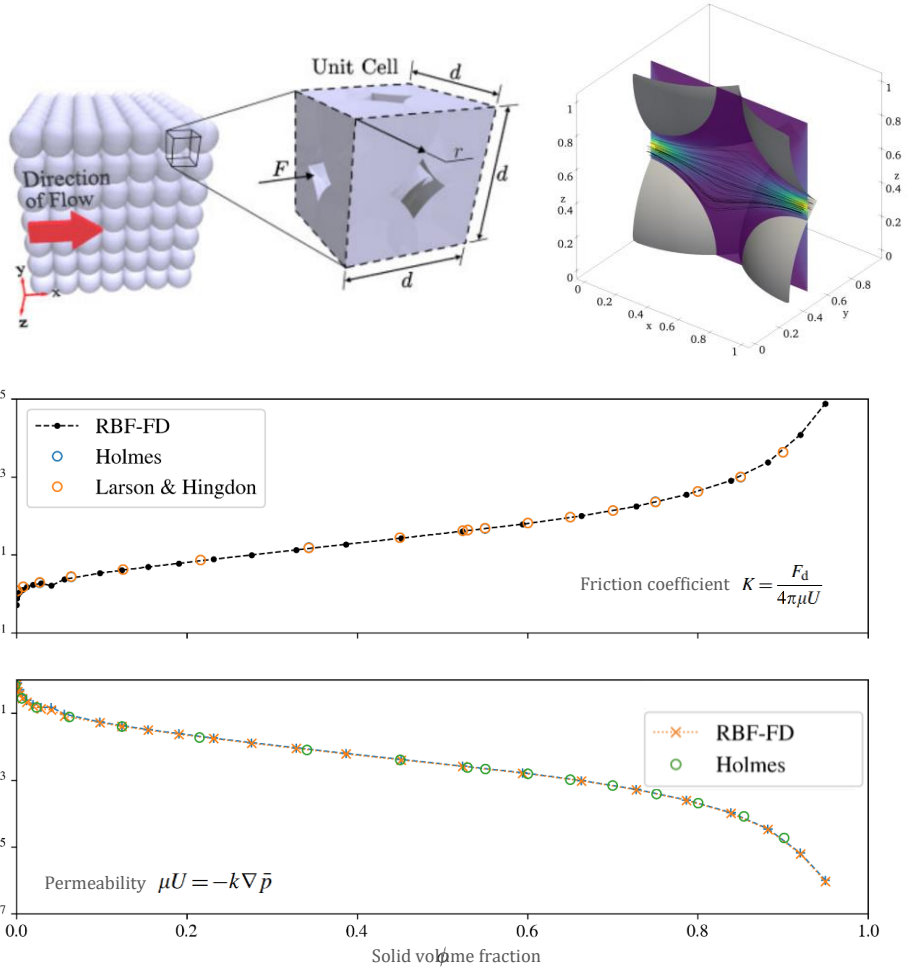

D. W. Holmes, J. R. Williams, P. Tilke, Smooth particle hydrodynamics simulations of low reynolds number flows through porous media, International Journal for Numerical and Analytical Methods in Geomechanics 35 (4) (2011) 419–437

Flow through disordered porous media
Randomly placed square obstructions on a 64x64 grid

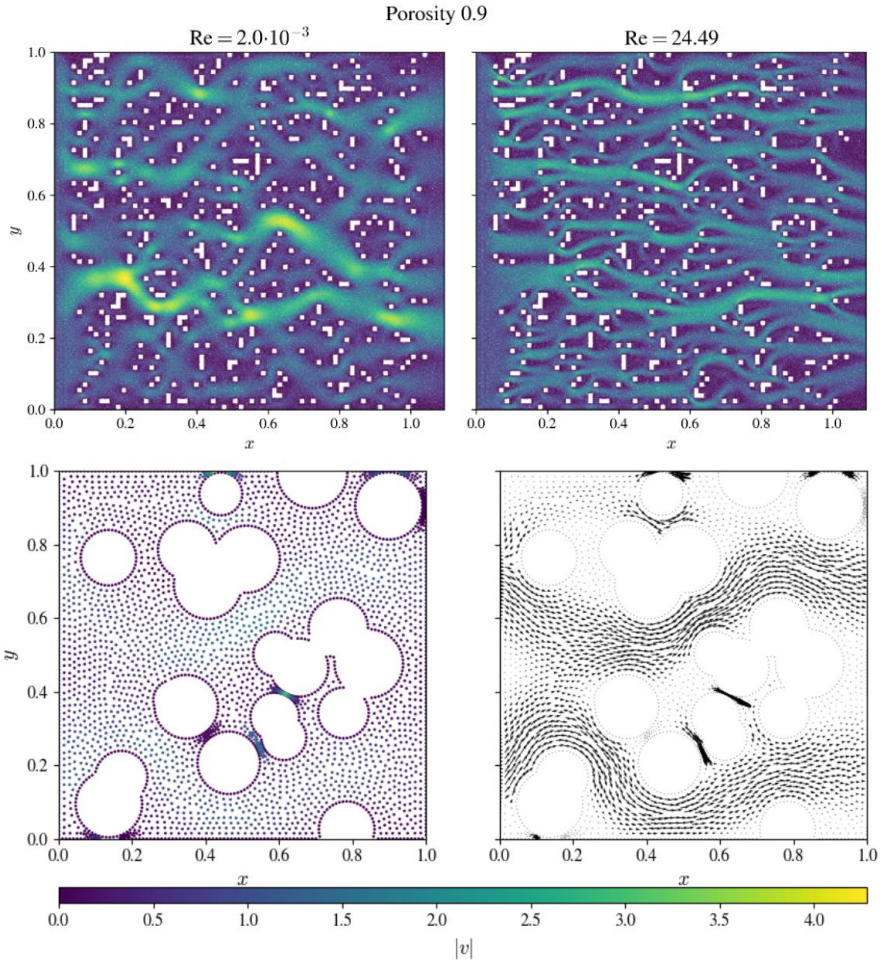

J.S. Andrade, U.M.S. Costa, M.P. Almeida, H.A. Makse, H.E. Stanley, Inertia effectson fluid flow through disordered porous media, The American Physical Society,Physical Review Letters 82 (26) (1999) 5249–5252.

Simulation of overhead power line cooling


Power plant


Transmission network


Distribution network


End users

The transfer capabilities of overhead power lines are limited by the critical power line temperature that depends on the magnitude of the transferred current and the ambient conditions.

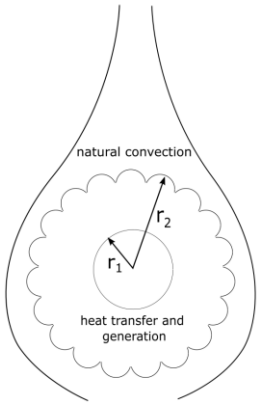

Natural convection problem:

$$\rho^a \frac{\partial \mathbf{v}}{\partial t} + \rho^a \nabla \cdot (\mathbf{v}\mathbf{v}) = -\nabla P + \nabla \cdot \left(\mu^a \nabla \mathbf{v}\right) + \mathbf{b}$$

$$\nabla \cdot \mathbf{v} = 0$$

$$\rho^a c_p^a \frac{\partial T^a}{\partial t} + \rho^a c_p^a \nabla \cdot (T^a \mathbf{v}) = \nabla \cdot \left(\lambda^a \nabla T^a\right)$$

Boundary condition

$$q_R = \sigma_B \epsilon_s \left(T_{al}^4(r_2) - T_a^4\right) \left[\frac{\mathrm{W}}{\mathrm{m}^2}\right]$$

$$q_S = \frac{\alpha_s I_T}{\pi} \left[\frac{\mathrm{W}}{\mathrm{m}^2}\right],$$

$$T^{al}(r_1) = T^{st}(r_1)$$

$$\lambda^{al} \left.\frac{\partial T^{al}}{\partial \mathbf{n}}\right|_{r_1} = \lambda^{st} \left.\frac{\partial T^{st}}{\partial \mathbf{n}}\right|_{r_1}$$

Heat transport and generation

$$c_p^{al} \rho^{al} \frac{\partial T^{al}}{\partial t} = \lambda^{al} \nabla^2 T^{al} + \frac{I^2 R\left(T^{al}\right)}{S^{al}}$$

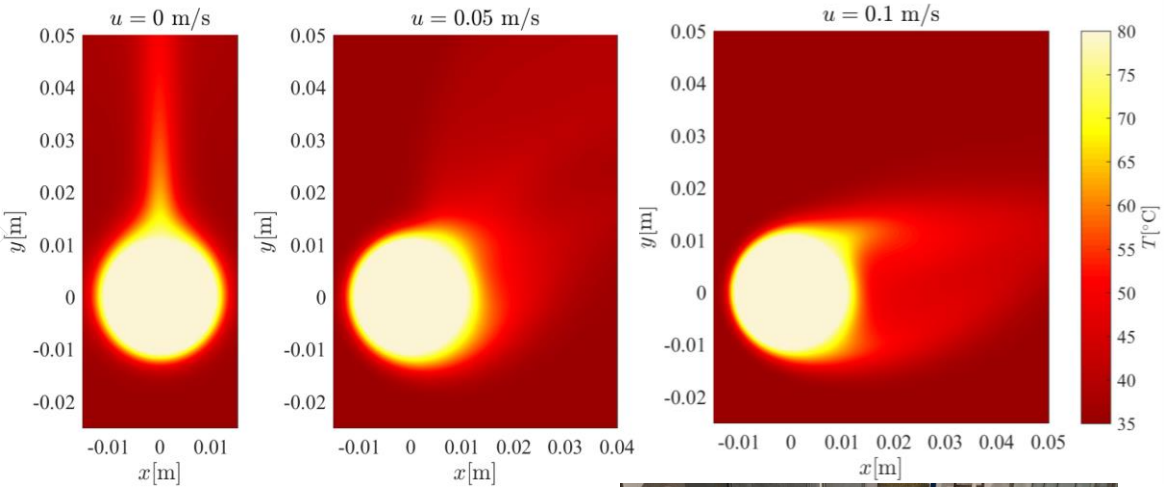

RBF-FD – numerical simulation, M - measurement

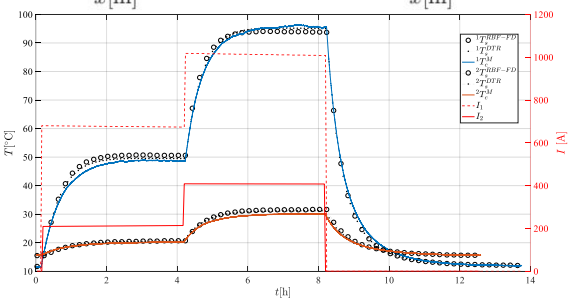

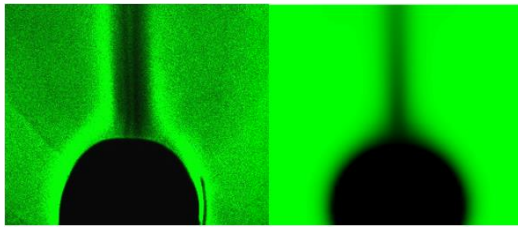
Result of Schlieren photography | Simulated temperature


Experimental setup

The project is funded by:

- ELES: transmitting energy, maintaining balance.

Dynamic thermal rating operational module

Extension and simplification of the model

Heat transfer within the conductor

$$\nabla\lambda\nabla T + q_i = \rho c_p \frac{\partial T}{\partial t}.$$

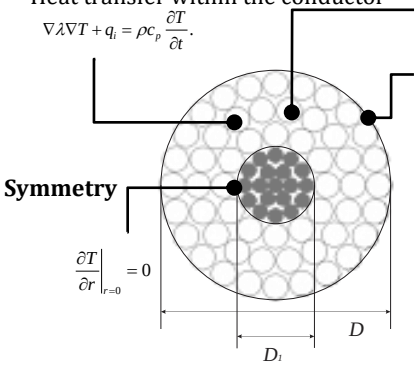

Heat generation

$$Q_J = I^2 R(T) \left[\frac{\mathrm{W}}{\mathrm{m}}\right]$$

Heat exchange with surrounding

Convection

$$Q_C = -\pi D h (T_s - T_a) \left[\frac{\mathrm{W}}{\mathrm{m}}\right]$$

Radiation

$$Q_R = -\pi D \sigma_B \epsilon_s (T_s^4 - T_a^4) \left[\frac{\mathrm{W}}{\mathrm{m}}\right]$$

Solar

$$Q_S = \alpha_s I_T D \left[\frac{\mathrm{W}}{\mathrm{m}}\right]$$

impinging

$$Q_{IM} = CED c_w \frac{d\rho_I}{dt}(T_S - T_I) \left[\frac{\mathrm{W}}{\mathrm{m}}\right]$$

evaporation

$$Q_E = -h \frac{\epsilon L_e A_w}{c_p} \left(\frac{e_s - e_a}{p}\right) \left[\frac{\mathrm{W}}{\mathrm{m}}\right]$$

Coupling with ALADIN model

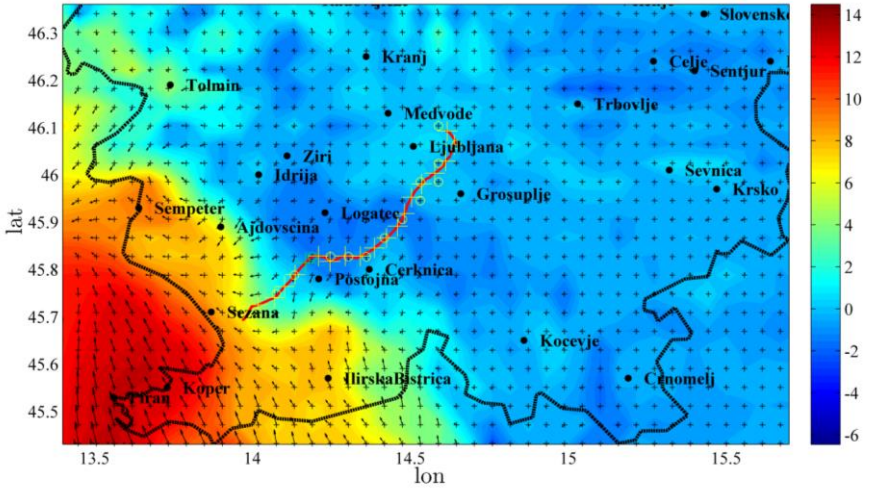

Validation

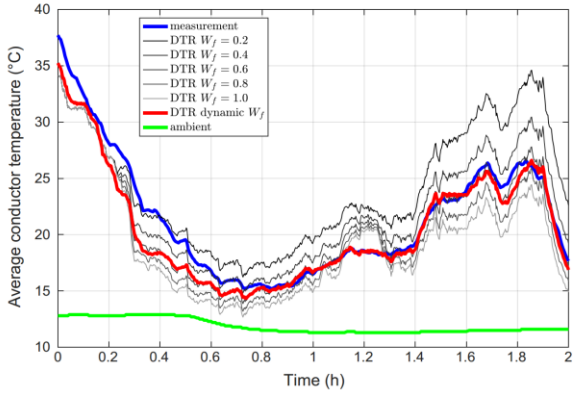

Comparison of simulated and measured line temperature at Podlog power line in August 2019.

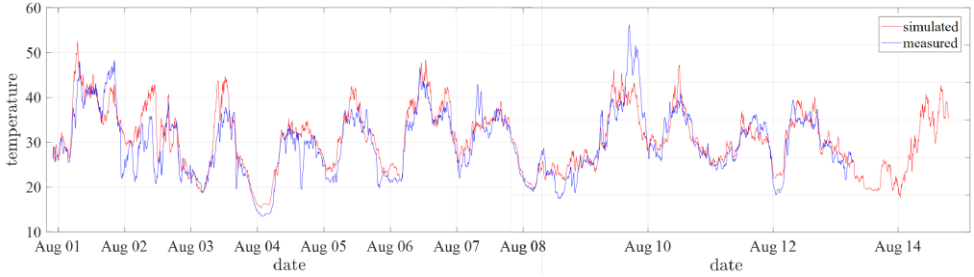

DTRi

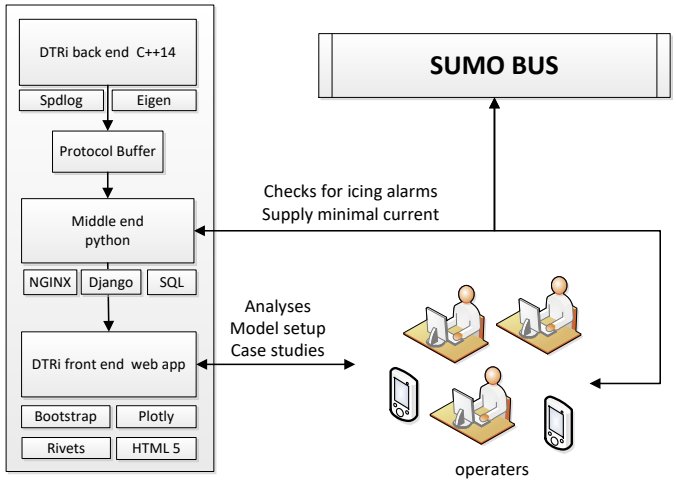

Mesh-free open source project Medusa

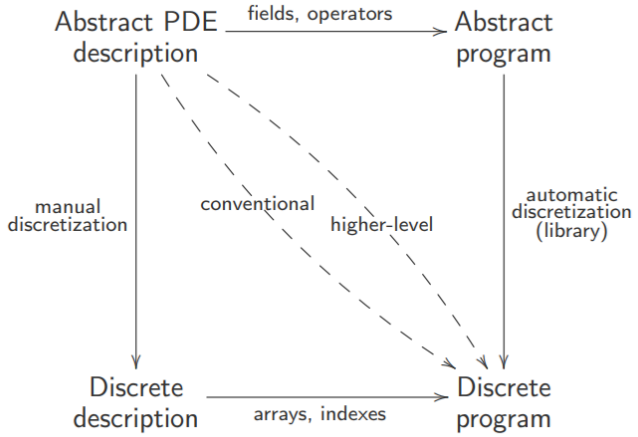

Main features:

- Modular design
- Coordinate free and dimension independent implementation
- Support different strong form meshless methods
- Explicit transformation of equations into code
- Minimal overheads due to the programming abstraction
- Tested code

Medusa is C++ template library using

- Eigen library for linear algebra
- Google test testing framework
- XML and HDF5 support for IO
- Nanoflann for spatial-search structures

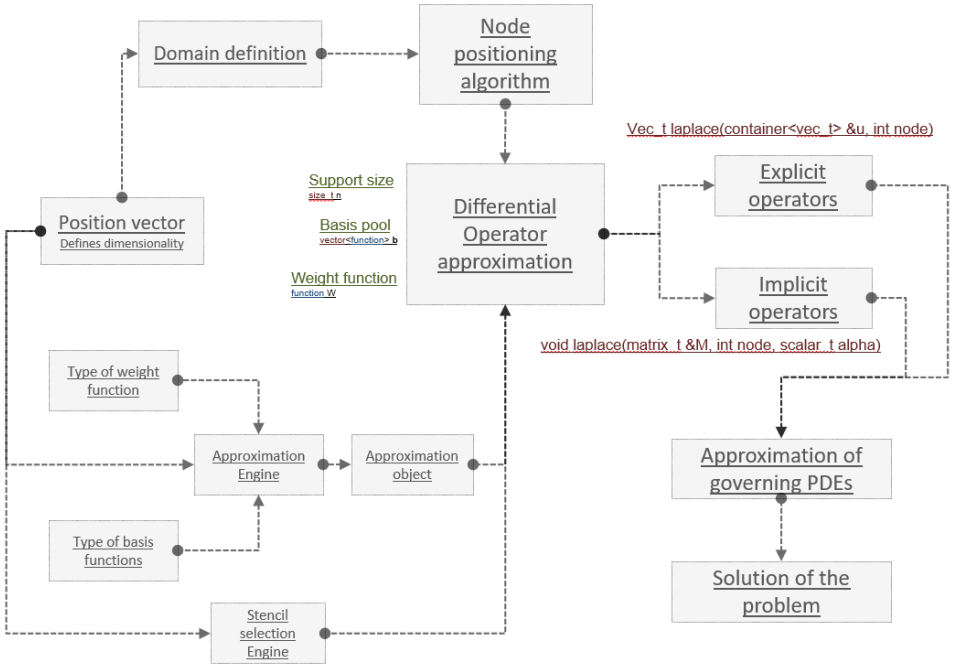

Doxygen http://e6.ijs.si/medusa/docs/html

MediaWiki http://e6.ijs.si/medusa/wiki/index.php/Medusa

GitLab https://gitlab.com/e62Lab/medusa

Conclusions

Meshless methods have some nice properties

- Simplified spatial discretisation
- Suitable for adaptive analysis

Medusa

- tested modular open source library for mesh-free simulations
- dimension independent
- explicit transformation of equations into code
- Supports hp – adaptivity

open source meshless project
Medusa: Coordinate Free Mehless Method implementation
https://gitlab.com/e62Lab/medusa
http://e6.ijs.si/medusa/

Future work

- Better marking strategy based on local data regularity
- Better understanding of the effect of the stencil size and shape on the accuracy and stability
- …

We are open for collaboration

- joint projects
- Student exchange
- Or just working together on fun problems

Thank you for your attention